The Cryosphere Discuss., 9, 6909–6936, 2015
www.the-cryosphere-discuss.net/9/6909/2015/
doi:10.5194/tcd-9-6909-2015

The Cryosphere
Discussions
Open Access

Non-climatic signal in ice core records: lessons from Antarctic mega-dunes

A. Ekaykin[1,2], L. Eberlein[3], V. Lipenkov[1], S. Popov[4], M. Scheinert[3], L. Schröder[3], and A. Turkeev[1]

[1]Climate and Environmental Research Laboratory, Arctic and Antarctic Research Institute, 38 Beringa st., 199397, St. Petersburg, Russia
[2]St. Petersburg State University, 33–35, 10th line VO, 199178 St. Petersburg, Russia
[3]Technische Universität Dresden, Institut für Planetare Geodäsie, 01062 Dresden, Germany
[4]Polar Marine Geological Research Expedition, 24 Pobedy st., 198412 Lomonosov, Russia

Received: 11 November 2015 – Accepted: 3 December 2015 – Published: 17 December 2015

Correspondence to: A. Ekaykin (ekaykin@aari.ru)

Published by Copernicus Publications on behalf of the European Geosciences Union.

Abstract

We present the results of glaciological investigations in the mega-dune area located 30 km to the east from Vostok Station (central East Antarctica) implemented during the 58th, 59th and 60th Russian Antarctic Expedition (January 2013–January 2015). Snow accumulation rate and isotope content (δD, δ^{18}O and δ^{17}O) were measured along the 2 km profile across the mega-dune ridge accompanied by precise GPS altitude measurements and GPR survey. It is shown that the spatial variability of snow accumulation and isotope content covaries with the surface slope. The accumulation rate regularly changes by one order of magnitude within the distance < 1 km, with the reduced accumulation at the leeward slope of the dune and increased accumulation in the hollow between the dunes. At the same time, the accumulation rate averaged over the length of a dune wave (22 mm we) corresponds well with the value obtained at Vostok Station, which suggests no additional wind-driven snow sublimation in the mega-dunes compared to the surrounding plateau. The snow isotopic composition is in negative correlation with the snow accumulation. Analyzing dxs/δD and 17O-excess/δD slopes, we conclude that the spatial variability of the snow isotopic composition in the mega-dune area could be explained by post-depositional snow modifications. Using the GPR data, we estimated the apparent dune drift velocity (4.6 ± 1.1 m yr^{-1}). The full cycle of the dune drift is thus about 410 years. Since the spatial anomalies of snow accumulation and isotopic composition are supposed to drift with the dune, an ice core drilled in the mega-dune area would exhibit the non-climatic 410 year cycle of these two parameters. We simulated a vertical profile of snow isotopic composition with such a non-climatic variability, using the data on the dune size and velocity. This artificial profile is then compared with the real vertical profile of snow isotopic composition obtained from a core drilled in the mega-dune area. We note that the two profiles are very similar. The obtained results are discussed in terms of interpretation of data obtained from ice cores drilled beyond the mega-dune areas.

1 Introduction

Mega-dunes are one of the most intriguing and spectacular phenomena in Antarctica. The first reports on the existence of the huge waves on the surface of the Antarctic ice sheet was made soon after the beginning of the extensive exploration of the Antarctic interior during the IGY (Dolgushin, 1958), although the term “mega-dunes” was not yet used at that time.

Since then such surface undulations have been observed in different parts of the Antarctic continent – in Adelie Land (Pettre et al., 1986), Dronning Maud Land (Anschütz et al., 2006; Eisen et al., 2005), Enderby Land (Fujita et al., 2002), Marie Byrd Land (Gow and Rowland, 1965; Whillans, 1975), Victoria Land (Frezzotti et al., 2002a, b), Queen Mary Coast (Dolgushin, 1958; Vladimirova and Ekaykin, 2014), Wilkes Land (Black and Budd, 1964; Goodwin, 1990) – or, simply speaking, almost everywhere.

In 1988 Swithinbank suggested to call such waves “mega-dunes” (Swithinbank, 1988) based on their similarity to the desert sand mega-dunes. At present this term is conventionally used to describe the specific dunes observed in central East Antarctica (Albert et al., 2004; Alberti and Biscaro, 2010; Arcone et al., 2012b; Fahnestock et al., 2000; Frezzotti et al., 2002b), which form the system of parallel ridges with the wavelength of 2–5 km, the amplitude 2–8 m, and the length of the ridges of up to 100 km.

The first observations of relationship between the ice sheet surface topography (surface slope) and snow accumulation rate have shown that the dunes strongly redistribute the snow with the increased accumulation in the concaves and reduced accumulation on the convexities (Black and Budd, 1964). This relationship has been later confirmed in a number of studies, e.g. Anschütz et al. (2007), Dadic et al. (2013), Ekaykin et al. (2002), Frezzotti et al. (2007), Fujita et al. (2011), Hamilton (2004), Kaspari et al. (2004), Richardson et al. (1997), Rotschky et al. (2004). These studies have also shown that the dunes are not stagnant, but rather drift across the ice sheet surface, which does not allow the snow to simply fill in the hollows between the dunes thus maintaining their dynamical equilibrium. The estimates of the dunes’ horizontal

Title Page
Abstract Introduction
Conclusions References
Tables Figures
◀ ▶
Back Close
Full Screen / Esc
Printer-friendly Version
Interactive Discussion

drift velocity ranges from 4 to 25 m yr^{-1} (Black and Budd, 1964; Frezzotti et al., 2002b; Van der Veen et al., 1999; Whillans, 1975).

The first dedicated ground survey of mega-dunes was made by Frezzotti et al. (2002b). It was shown, in particular, that snow is removed from the leeward slopes of the dunes where specific erosional type of snow, "glaze surface", is formed. In contrast, snow accumulation is increased on the windward slopes that are characterized by the depositional types of the snow microrelief.

Since the 1980s the mega-dunes are observed with the use of the satellite methods (Alberti and Biscaro, 2010; Fahnestock et al., 2000; Scambos et al., 2012; Swithinbank, 1988), which has revealed that these snow features are widely presented in Antarctica occupying in total about 500 000 km^2.

The Antarctic glaciology has gained a lot from implementing the ground penetrating radar (GPR) technique (Eisen et al., 2008). The GPR survey has also been made in mega-dune areas (Anschütz et al., 2006; Arcone et al., 2012a, b; Eisen et al., 2005; Frezzotti et al., 2002a). In particular, this allowed discovering the mega-dune-like structures in the central Antarctica outside the "classical" mega-dune areas. Similar to mega-dunes, they are characterized by persistent zones of snow erosion (glaze surfaces) and increased accumulation. The disturbed stratigraphy that marks the buried glaze surfaces is found at the depths more than 2000 m, which suggests that these structures have been persistent for tens of thousands of years (Arcone et al., 2012a, b).

The precipitated snow is not simply re-distributed in the mega-dune area. Indeed, it is widely recognized that the wind-driven sublimation is an important part of the surface snow mass-balance (Bintanja and Reijmer, 2001; Lenaerts et al., 2010; Thiery et al., 2012) removing from 20 to 75 % of precipitation (Frezzotti et al., 2004, 2007). In the mega-dunes this figure may increase to 85 % (Frezzotti et al., 2004).Thus, the wide extent of the mega-dune fields and glaze surfaces (that occupy in total more than 10 % of the continent area), where snow drift processes are intensified, must be taken into account for correct estimate of the Antarctic surface mass balance (Das et al., 2013; Scambos et al., 2012; Zwally et al., 2015).

Physical properties of snow in the mega-dune areas have been studied by Albert et al. (2004), Courville et al. (2007), Gregory et al. (2014), Severinghaus et al. (2010). In particular, the snow erosion zones of mega-dunes are represented by coarse-grained snow (depth hoar) characterized by increased air permeability. The processes taking place in snow under near-zero accumulation help to understand the data on isotopic composition of gas trapped in the ice core air bubbles (Severinghaus et al., 2010). It is suggested that low-accumulation highly permeable snow zones, similar to that currently existing in the mega-dune areas, had large extent in Antarctica in the glacial times (Dreyfus et al., 2010).

Chemical properties of the mega-dune snow were considered in very few studies (Dixon et al., 2013). It is noted that the surface slope may, at least in the coastal areas, affect the snow chemistry (Mahalinganathan et al., 2012).

The strong post-depositional metamorphosis of snow in the mega-dunes has to modify its stable water isotope properties (Courville et al., 2007; Frezzotti et al., 2002b; Neumann et al., 2005). It is also known that irregular snow redistribution by wind due to complex surface topography does affect the isotopic content of the deposited snow, which cause a poor correlation of isotopic profiles obtained in two points separated by only a short distance (Benoist et al., 1982; Ekaykin et al., 2014; Karlöf et al., 2006). However, no systematic study of snow isotopic composition in the mega-dunes has been conducted up to now.

In the summer seasons of 58th, 59th and 60th Russian Antarctic Expeditions (RAE), 2013–2015, we carried out complex glaciological investigations in the mega-dune area located about 30 km to the East from Russian Vostok Station (Fig. 1). In this paper we analyze the spatial distribution of the snow isotope content in the mega-dunes.

2 Data and methods

2.1 Glaciological and stable water isotope data

In January 2013 the Vostok mega-dune area was visited for the first time. The accumulation-stake profile was established perpendicular to the mega-dune crest. The total number of stakes was 21 (named MD00 to MD20), the distance between adjacent stakes was about 100 m, and the total length of the profile was 1983 m (Fig. 1). The samples of the upper 1.5 m of snow were also taken near each stake to be analyzed for the concentration of the stable water isotopes (δD, δ^{18}O and δ^{17}O).

In January 2014 and January 2015 the stakes were revisited, and the repeated measurements of their heights and surface snow density allowed obtaining the amount of snow accumulated during 2 years (January 2013–January 2015). The snow samples were taken again for chemical and isotopic analyses.

In January 2015 we also drilled a 20 m borehole in point MD00 (Fig. 1). In the obtained firn core we measured snow density and took samples for stable water isotope analysis with a resolution of 10 cm.

The concentration of heavy water isotopes (δD and δ^{18}O) in 42 snow surface samples taken in 58th and 59th RAE, as well as in 183 samples from MD00 core, was measured at Climate and Environmental Research Laboratory (CERL) using a Picarro L2120-*i* analyzer. Our working standard (VOS), measured after every 5 samples, was made of the light Vostok snow and calibrated against the IAEA standards VSMOW-2, GISP and SLAP-2. The reproducibility of results defined by re-measurements of randomly chosen samples was 0.04 ‰ for δ^{18}O and 0.2 ‰ for δD, which is 2 orders of magnitude less than the natural variability of the snow isotopic composition (see below) and thus satisfactory for the purposes of the study.

In October 2015 we also measured 17O-excess values in the samples collected during the 59th RAE using a Picarro L2140-*i* analyzer. For this, each sample was measured 15 times in the high-precision mode and we took an average of the last 10 measurements. Every 3 samples we measured the VOS standard previously calibrated against VSMOW-2, GISP and SLAP-2 (taking into account that they have 17O-excess values of, correspondingly, 0, 22 and 0 per meg; Schoenemann et al., 2013). The 17O-excess value of VOS was found to be 0 per meg, similar to SLAP. The reproducibility of the 17O-excess values of individual samples was 8 per meg.

All the data discussed in this paper is presented in Table 1.

2.2 GNSS positioning

The absolute altitude and location was determined with high accuracy along the profile using the geodetic GPS technique.

Therefore the Bernese GPS Software 5.1 (Dach et al., 2007) was used to process the two kinematic GNSS profiles (K58B and K58C) as a combined differential solution from GPS and GLONASS observations. As reference stations for this network solution we used two local receivers at Vostok station in a distance of less than 50 km and additional two reference stations at the coast with baseline lengths of about 1350 km (near the Russian research stations Progress and a station of the global IGS-network near the Australian Station Casey). After reducing the antenna positions to the snow surface we estimated the accuracy by calculating the height differences at track crossovers. Crossovers inside one track imply an internal RMS of the differences of 2.9 cm (at 160 crossover points) for track K58B and 2.4 cm (at 9 crossover points) for track K58C. With a RMS of 7.7 cm at 5159 crossovers between the two tracks we can estimate the absolute precision of a single kinematic surface height according to the variance propagation to about 5.4 cm.

2.3 GPR data

During the austral summer field season of the 58th Russian Antarctic Expedition (January 2013) the GPR profiling was performed to study the snow-firn layer structure of the mega-dune area. The 200 MHz GSSI SIR10B GPR with “5106 200 MHz” antenna was applied.

The GPR equipment was installed on 2 sledges towed by a ski-doo. The route of the GPR profiling was the same with the geodetic observations. In total, about 80 km of the GPR profiles were obtained (Fig. 1), though in this paper we only use the 2 km section obtained along the glaciological profile (points MD00-MD20 in Fig. 1).

The main problem in the processing and interpretation of the GPR data is the dielectric properties of the media where the electromagnetic waves are propagating. We used the model published by Popov and Eberlein (2014) to transform the radio-echo time-section (Fig. 2) into the depth section. To calculate the vertical electromagnetic wave speed we used the firn density data measured in MD00 core.

In Fig. 2 we showed the GPR registration recorded along the glaciological profile (MD00-MD20).

3 Results

The mega-dune formation is related to a sharp increase of the ice sheet slope in the prevailing wind direction (SPWD) (Frezzotti et al., 2002b). The Vostok mega-dunes are not an exception, as they form leeward from the eastern shore of the Lake Vostok, where the SPWD changes from near zero or even negative values (interestingly, in the closest vicinities of Vostok Station the wind is blowing uphill) to about 1.6 m km^{-1}. The latter figure generally agrees with the Frezzotti et al. (2002) conclusion that the mega-dunes only develop where the SPWD is from 1 to 1.5 m km^{-1}.

The wavelength of the Vostok mega-dunes are about 1.9 km, and the amplitude (the elevation change between the dune crest and the nearest windward hollow) is about 1.2 m, i.e. they are relatively small compared to those reported in the above mentioned studies.

Below we present the results of the glaciological investigations in the Vostok mega-dune area (Fig. 3).

3.1 Accumulation rate and isotopic content of snow in mega-dunes

Due to the subsequent measurements of the heights of the stakes established across the mega-dunes, we were able to define the snow accumulation between January 2013 and January 2015 (Fig. 3e). One may clearly see the regular spatial variability of the snow build-up. In accordance with the previous studies (see the review in Introduction), the snow is removed from locations with the increased surface slope (leeward side of the dunes) and deposited where the slope is decreased or inversed (hollow between dunes and windward side of the dunes). In a distance of few hundred meters the accumulation changes by an order of magnitude, from −0.5 to 16 cm of snow (or from −0.2 to 58 mm we according to the surface snow density, Fig. 3d). This range is larger than that reported by Frezzotti et al. (2002b) (from 7 to 35 mm). The mean annual accumulation over the 1 dune wavelength is 22 mm, which is very similar to the accumulation at the Vostok stake network (23 mm). If the precipitation rate at Vostok station and in the mega-dune area was the same, then our result does not support the observation that over the mega-dune areas the accumulation is reduced due to the wind-driven sublimation (Frezzotti et al., 2004).

The surface snow density does not show any distinct spatial variability (Fig. 3d). The mean snow density (0.355 g cm^{-3}) is slightly higher than that measured at Vostok stake network (0.33 g cm^{-3}).

During the field-works we also did not observe big difference between snow surface character in leeward and windward slopes of the dunes (Fig. 4). The erosion zone does not demonstrate the dominance of the glaze surface, and no big sastrugi are observed in the accumulation zone, as reported by Frezzotti et al. (2002b) for the Victoria Land mega-dune field.

The spatial variability of the accumulation rate covaries well with the surface slope: the smaller is the slope, the higher is accumulation (Fig. 3f and e), in accordance with the previous observations (Anschütz et al., 2006).

In Fig. 3a–c we show the isotopic composition (δD, dxs and 17O-excess) of the upper 1.5 m of snow sampled twice near each point of our profile. One can see a wave in snow isotopic content (δD) with the magnitude of about 20 ‰ and the wavelength similar to that of the mega-dune. There is a negative covariation between snow isotopic composition and accumulation rate (correlation coefficient, −0.38, is not statistically significant due to the small number of points). A very similar picture was previously observed in the closest vicinity of Vostok, where positive spatial anomalies of isotopic composition correspond to the negative anomalies of snow accumulation, though on the smaller spatial scale (Ekaykin et al., 2002).

We explain this behavior of the snow isotopic composition by different post-depositional alteration of the initial isotopic composition of snow precipitation deposited in the low- and high-accumulation zones of the mega-dunes. Indeed, the erosion zone is characterized by “a long, multiannual, steep temperature-gradient metamorphism” (Frezzotti et al., 2002b, p. 8). Thus, the snow here should be enriched in heavy isotopes due to strong post-depositional modification (Town et al., 2008) that may be further facilitated by the increased permeability of the snow in such locations (Albert et al., 2004). We may speculate that in the mega-dunes described by Frezzotti et al. (2002b), characterized by a very strong modification of the snow physical properties, the isotopic transformation should be even stronger than in the Vostok dunes.

An alternative explanation of negative spatial relationship of isotopic composition and snow accumulation was suggested by Ekaykin et al. (2002). Since in winter the snow crystals are smaller and wind speed is higher, this snow could be easier re-distributed by wind comparing to snow precipitated in summer. If so, in the erosion zone of the mega-dunes the proportion of summer snow is larger than in the accumulation zone.

We may use the isotopic data to determine which mechanism, “post-depositional” or “re-distributional” (or both) is mainly responsible for the anomaly of the snow isotopic composition in the mega-dune area.

The observed dxs/δD and 17O-excess/δD slopes (ratios between the standard deviations of the smoothed profiles shown in Fig. 3a–c) are, correspondingly, −0.2 ‰/‰

and 0.9 per meg/‰. During the post-depositional changes of the snow isotopic composition these slopes are −0.2 ‰/‰ and 0.4 per meg/‰ (Ekaykin et al., 2016). During the seasonal cycle of the isotopic composition of snow precipitation at Vostok, these parameters are related by slopes −0.1 ‰/‰ and 0.4 per meg/‰ (Landais et al., 2012).

Thus we may conclude that the mixing of the summer and winter precipitation in different proportions cannot explain the variability of snow isotopic composition observed in the mega-dune area, since the variability of 17O-excess and of dxs would be significantly smaller. The post-depositional factor would better explain the observed snow isotopic composition in the mega-dunes, but still the variability of 17O-excess seems to be too strong. Note, however, that the data of Ekaykin et al. (2016) were obtained in laboratory experiments, not in natural conditions, so the 17O-excess/δD slopes reported there may be underestimated.

We should also note that the 17O-excess values positively covariate with the accumulation rate (Fig. 3c and e), though one would expect a negative covariation in case if the snow isotopic composition variability is due to the post-depositional processes. At present we do not know if this positive covariation is caused by errors in the 17O-excess values, or it suggests another mechanism that creates isotopic anomalies in the mega-dune area.

3.2 Mega-dune drift

We used the GPR data to reconstruct the previous positions of the dunes, and to calculate the velocity of the dunes drift.

In the GPR profile taken across the mega-dunes (Fig. 2), we see several distinct internal reflection horizons (IRH). For 7 of them we defined the depths (Table 1) and, subtracting these depths from the ice sheet elevation, we could define the absolute altitude of each IRH (Fig. 3g). Thus we can see the buried surfaces of our dune and may trace its drift in time.

For this, we first need to date each IRH. We used the density profile obtained from the MD00 core and the average snow accumulation rate in the mega-dune area in order to calculate the depth-age function and determine the age of each IRH (Fig. 3g). The uppermost IRH marks the surface of the dune about 130 years ago, and the lowermost – 530 years ago.

We chose 3 fold hinges (the summit of crests and two lowest points of the fold dips) to trace the dune drift. On average, the dune is drifting upwind with the rate of $4.6 \pm 1.1\,\mathrm{m\,yr^{-1}}$. This corresponds very well with the value reported by Frezzotti et al. (2002b), $5\,\mathrm{m\,yr^{-1}}$. With this velocity a dune drift by 1 wavelength in about 410 years.

As pointed by Arcone et al. (2005), the apparent dune drift velocity observed in the GPR images is a combination of the real dune velocity and the ice movement, and the real dune velocity is higher than the observed one. According to Richter et al. (2013), ice flow velocities in this region do not exceed $2\,\mathrm{m\,yr^{-1}}$, so the real dune drift velocity could be up to $6.6\,\mathrm{m\,yr^{-1}}$. However, the ice is moving almost in parallel with the dune crests (from north-west to south-east). So, the projection of the ice speed vector on the MD profile is close to $0\,\mathrm{m\,yr^{-1}}$, and the correction to the dune drift velocity due to the ice movement should be close to zero, too. Finally, for the purposes of our study we need not real, but the resultant dune velocity observed by GPR, so in the further calculations we use the apparent dune velocity of $4.6\,\mathrm{m\,yr^{-1}}$.

3.3 Non-climatic temporal oscillation related to the mega-dune drift

When the dune drifts, the spatial anomalies in snow physical properties, accumulation rate and isotopic composition are drifting accordingly. For example, the point MD00, now located at the leeward side of the dune with reduced accumulation and enriched isotopic composition, about 300 years ago was in the hollow between dunes with increased accumulation and lower heavy isotope content. If one drills an ice core in the mega-dune area, he would see a quasi-periodic (with the period of 410 years) oscillations in snow accumulation and isotopic composition related to the dune drift.

Let us simulate such an oscillation that we would see in a core drilled at MD00 point.

In Fig. 5a we showed a temporal variability of snow accumulation (blue) and isotopic composition (red) that should be seen in point MD00 when the dune crosses this point. To construct these curves, we simply divided the distance of each point in Fig. 3a and e by the above mentioned velocity of the dune drift. We also showed in Fig. 5a the climatic variability in Vostok region over the same time interval (Ekaykin et al., 2014) in purple. Note that the amplitudes of the both components are similar.

Combining the dune-related and climatic components, we obtain the expected temporal variability of snow isotopic composition in MD00 (Fig. 5b). Then we transform it to a vertical isotopic profile using the depth-age function presented in Fig. 5c. This function takes into account the significant dune-related variability in snow accumulation rate (Fig. 5a), this is why it is essentially non-linear. The resulting simulated vertical isotopic profile is presented in Fig. 5d by red line. In the upper part of the profile the isotopic oscillations are compressed due to the low accumulation rate, and deeper, when the accumulation is higher, they are stretched.

In our simulations we do not take into account that the mega-dune snow may experience enhanced diffusive smoothing due to the increased ventilation of the snow column. In this case the isotopic profile could be substantially smoothed.

In Fig. 5d we also showed by the blue line the real isotopic profile from the MD00 core. One can see a good resemblance between them, except for the very bottom part of the MD00 core. Indeed, at the depth of 20 m the core has isotopic composition of −420 ‰. Neither climatic record, nor the isotopic profile from the mega-dunes (Fig. 5a) demonstrate such high isotopic value, this is why we could not reproduce it in our simulations.

4 Discussion – non-climatic variability in ice cores

In the previous sections we demonstrated that the snow isotopic composition has significant spatial variability in the mega-dune area, suggested a possible mechanism to explain this variability, and then explained how this “dune-related” signal is transferred to an ice core isotopic profile. We calculated an artificial ice core isotopic profile in the mega-dune area and compared it with the real ice core isotopic profile.

In the case of MD00 core we know that the "signal" we see is mostly related to a dune drift, but how can one separate the climatic signal from non-climatic variability in real ice cores?

Indeed, it is commonly understood that a mega-dune area is an unsuitable place to drill ice for climatic studies, but it does not mean that the locations outside the mega-dune fields are free from non-climatic, "relief-related" variability.

As an example we may mention the South Pole Station region that is not a mega-dune area, but detailed topographic survey shows mega-dune-like features with a typical amplitude of few meters and wavelength of several kilometers – see Fig. 8 in Van der Veen et al. (1999) and Fig. 2 in Hamilton (2004). Unlike the mega-dunes, these snow hills are not elongated, but rather round in shape. The authors suggest these structures are not stationary, but slowly change their locations, which causes temporal non-climatic variability of snow accumulation rate with the period of several hundred or few thousand years. Very similar structures are observed around the Kohnen Station (Eisen et al., 2005) and in West Antarctica (Arcone et al., 2005).

Even the vicinities of the main domes cannot be considered as "dune-safe". Indeed, the study of the snow isotopic composition profile in two neighboring cores drilled at Dome C showed a very low signal-to-noise ratio likely related to the local ice sheet topography (Benoist et al., 1982).

In Dronning Maud Land the ice cores drilled in relatively short distance one from another demonstrate opposite trends in the snow accumulation rates over the past 200 years (Oerter et al., 2000), which may be considered as the influence of the non-climatic factors.

In general, in low-accumulation sites signal-to-noise ratio in both snow accumulation rate and isotopic composition is very small, being of the order of 0.2 (Ekaykin et al., 2014). The noise, related to the snow re-distribution by wind and/or post-depositional processes, is larger than the climatic signal even at the centennial scale. This means that to study climatic variability with the periods less than 10^3–10^4 years in the low accumulation area (which comprises most of the East Antarctica (Arthern et al., 2006)) more than one ice core should be investigated for each location.

The influence of snow topography on snow accumulation is known and to large extent understood on the spatial scale from 10^{-2} to 10^1 m (micro-relief) and from 10^3 to 10^6 m (mega-dunes and continental scale). However, very little is known about the scale from 10^1 to 10^3, the range of “meso-dunes” (Eisen et al., 2008; Ekaykin et al., 2002). It is likely that the drift of the meso-dunes causes the non-climatic temporal oscillations of snow isotopic composition and accumulation rate with a period of few tens of years due to mechanisms similar to those described in this paper for the mega-dunes. Further studies of this phenomenon are needed.

5 Conclusions

The ice cores are priceless source of numerous and diverse paleo-climatic data, and this will hold true even despite the unavoidable limitations. One of the most important limitations is related to a high level of noise which contaminates the climatic signal on relatively short time scales (years to millennia), especially in the low-accumulation areas. The main reason of this noise is a complex snow/ice sheet topography that leads to snow re-distribution due to wind activity, which is further complicated by the post-depositional processes.

In this paper we present the results of the field works carried out during three Antarctic summer seasons in the vicinity of Vostok Station. We mainly deal with the influence of large snow relief forms, mega-dunes, on the snow isotopic composition. We demonstrate that the leeward sides of the dunes are characterized by reduced accumulation and increased concentration of heavy water molecules likely due to post-depositional alteration of the snow isotopic content. In opposite, windward sides of the dunes accumulate more snow that is enriched in light water isotopes.

Using the GPR data, we were able to trace the drift of the dunes and to calculate their velocity, $4.6 \pm 1.1\,\mathrm{m\,yr^{-1}}$. This allowed us to simulate the temporal variability of the snow isotopic composition that would be observed in a given point due to the passing of the mega-dune across this point. Then we compared this artificial vertical profile of the snow isotopic composition with the real isotopic data from a firn core drilled in the mega-dune cite. We showed that the two profiles are very similar.

Using the examples published in literature we suggest that similar non-climatic oscillations in snow accumulation rate and isotopic composition are widespread in Antarctica, even beyond the mega-dune fields.

We also suggest that the mega-dunes are a unique environment that provides the necessary conditions to test different hypothesis. For example, in a short distance one can find locations absolutely different in terms of snow accumulation rate, isotopic composition, physical and (likely) chemical properties, which could be used to study the post-depositional processes, to model glacial conditions (Severinghaus et al., 2010) etc.

In the future studies we plan to investigate the spatial variability of chemical content, the concentration of microparticles and other compounds in the surface snow in the Vostok mega-dune area.

Acknowledgements. The logistic operations in Antarctica were provided by Russian Antarctic Expedition. We personally thank Vitaly Zarovchatskiy for his help in the field works. The authors are grateful to Anna Kozachek and Diana Vladimirova (CERL) for the high-quality isotopic data. We also thank Achille Zirizzotti and Stefano Urbini (Istituto Nazionale di Geofisica e Vulcanologia, Rome, Italy) for providing the GPR equipment.

This study was completed at the expense of the grant of Russian Science Foundation (project 14-27-00030).

References

Albert, M., Shuman, C., Courville, Z., Bauer, R., Fahnestock, M., and Scambos, T.: Extreme firn metamorphism: impact of decades of vapor transport on near-surface firn at a low-accumulation glazed site on the East Antarctic Plateau, Ann. Glaciol., 39, 73–78, 2004.

Alberti, M. and Biscaro, D.: Height variation detection in polar regions from icesat satellite altimetry, Comput. Geosci., 36, 1–9, 2010.

Anschütz, H., Eisen, O., Rack, W., and Scheinert, M.: Periodic surface features in coastal East Antarctica, Geophys. Res. Lett., 33, 1–5, 2006.

Anschütz, H., Eisen, O., Oerter, H., Steinhage, D., and Scheinert, M.: Investigating small-scale variations of the recent accumulation rate in coastal Dronning Maud Land, East Antarctica, Ann. Glaciol., 46, 14–21, 2007.

Arcone, S. A., Spikes, V. B., and Hamilton, G. S.: Stratigraphic variation within polar firn caused by differential accumulation and ice flow: interpretation of a 400 MHz short-pulse radar profile from West Antarctica, J. Glaciol., 51, 407–422, 2005.

Arcone, S. A., Jacobel, R., and Hamilton, G.: Unconformable stratigraphy in East Antarctica: Part II. Englacial cosets and recrystallized layers, J. Glaciol., 58, 253–264, 2012a.

Arcone, S. A., Jacobel, R., and Hamilton, G.: Unconformable stratigraphy in East Antarctica: Part I. Large firn cosets, recrystallized growth, and model evidence for intensified accumulation, J. Glaciol., 58, 240–252, 2012b.

Arthern, R. J., Winebrenner, D. P., and Vaughan, D. G.: Antarctic snow accumulation mapped using polarization of 4.3-cm wavelength microwave emission, J. Geophys. Res., 111, D06107, doi:10.1029/2004JD005667, 2006.

Benoist, J. P., Jouzel, J., Lorius, C., Merlivat, L., and Pourchet, M.: Isotope climatic record over the last 2.5 ka from Dome C, Antarctica, ice cores, Ann. Glaciol., 3, 17–22, 1982.

Bintanja, R. and Reijmer, C. H.: A simple parameterization for snowdrift sublimation over Antarctic snow surfaces, J. Geophys. Res., 106, 31739–31748, 2001.

Black, H. P. and Budd, W.: Accumulation in the region of Wilkes, Wilkes Land, Antarctica, J. Glaciol., 5, 3–15, 1964.

Courville, Z. R., Albert, M. R., Fahnestock, M. A., Cathles IV, L. M., and Shuman, C. A.: Impacts of an accumulation hiatus on the physical properties of firn at a low-accumulation polar site, J. Geophys. Res., 112, 1–11, 2007.

Dach, R., Hugentobler, U., Fridez, P., and Meindl, M.: Bernese GPS Software Version 5.0, Univ. of Bern, Bern, Switzerland, 2007.

Dadic, R., Mott, R., Horgan, H. J., and Lehning, M.: Observations, theory, and modeling of the differential accumulation of Antarctic megadunes, J. Geophys. Res.-Earth, 118, 2343–2353, doi:10.1002/2013JF002844, 2013.

Das, I., Bell, R. E., Scambos, T. A., Wolovick, M., Creyts, T. T., Studinger, M., Frearson, N., Nicolas, J. P., Lenaerts, J. T. M., and Van den Broeke, M. R.: Influence of persistent wind scour on the surface mass balance of Antarctica, Nat. Geosci., 6, 367–371, 2013.

Dixon, D. A., Mayewski, P. A., Korotkikh, E., Sneed, S. B., Handley, M. J., Introne, D. S., and Scambos, T. A.: Variations in snow and firn chemistry along US ITASE traverses and the effect of surface glazing, The Cryosphere, 7, 515–535, doi:10.5194/tc-7-515-2013, 2013.

Dolgushin, L. D.: Geographical observations in Antarctica, Rep. 1, Izv. AN SSSR, Geography, 1, 28–47, 1958.

Dreyfus, G., Jouzel, J., Bender, M., Landais, A., Masson-Delmotte, V., and Leuenberger, M.: Firn processes and δ^{15}N: potential for a gas-phase climate proxy, Quaternary Sci. Rev., 29, 28–42, 2010.

Eisen, O., Rack, W., Nixdorf, U., and Wilhelms, F.: Characteristics of accumulation around the EPICA deep-drilling site in Dronning Maud Land, Antarctica, Ann. Glaciol., 41, 41–46, 2005.

Eisen, O., Frezzotti, M., Genthon, C., Isaksson, E., Magand, O., Van den Broeke, M. R., Dixon, D. A., Ekaykin, A. A., Holmlund, P., Kameda, T., Karlöf, L., Kaspari, S., Lipenkov, V. Y., Oerter, H., Takahashi, S., and Vaughan, D. G.: Ground-based measurements of spatial and temporal variability of snow accumulation in East Antarctica, Rev. Geophys., 46, 1–39, 2008.

Ekaykin, A. A., Lipenkov, V. Y., Barkov, N. I., Petit, J. R., and Masson-Delmotte, V.: Spatial and temporal variability in isotope composition of recent snow in the vicinity of Vostok Station: implications for ice-core interpretation, Ann. Glaciol., 35, 181–186, 2002.

Ekaykin, A. A., Kozachek, A. V., Lipenkov, V. Y., and Shibaev, Y. A.: Multiple climate shifts in the Southern Hemisphere over the past three centuries based on central Antarctic snow pits and core studies, Ann. Glaciol., 55, 259–266, 2014.

Ekaykin, A. A., Hondoh, T., Lipenkov, V. Y., Miyamoto, A., and Barkan, E.: Laboratory measurements of the impact of sublimation on post-depositional changes in snow isotope content, Clim. Past, submitted, 2016.

Fahnestock, M. A., Scambos, T. A., Shuman, C. A., Arthern, R. J., Winebrenner, D. P., and Kwok, R.: Snow megadune fields on the East Antarctic Plateau: extreme atmosphere-ice interaction, Geophys. Res. Lett., 27, 3719–3722, 2000.

Frezzotti, M., Gandolfi, S., La Marca, F., and Urbini, S.: Snow dunes and glazed surfaces in Antarctica: new field and remote-sensing date, Ann. Glaciol., 34, 81–87, 2002a.

Frezzotti, M., Gandolfi, S., and Urbini, S.: Snow megadunes in Antarctica: sedimentary structure and genesis, J. Geophys. Res., 107, 4344, doi:10.1029/2001JD000673, 2002b.

Frezzotti, M., Pourchet, M., Flora, O., Gandolfi, S., Gay, M., Urbini, S., Vincent, C., Becagli, S., Gragnani, R., Proposito, M., Severi, M., Traversi, R., Udisti, R., and Fily, M.: New estimations of precipitation and surface sublimation in East Antarctica from snow accumulation measurements, Clim. Dynam., 23, 803–813, 2004.

Frezzotti, M., Urbini, S., Proposito, M., Scarchilli, C., and Gandolfi, S.: Spatial and temporal variability of surface mass balance near Talos Dome, East Antarctica, J. Geophys. Res., 112, 1–15, 2007.

Fujita, S., Maeno, H., Furukawa, T., and Matsuoka, K.: Scattering of VHF radio waves from within the top 700 m of the Antarctic ice sheet and its relation to the depositional environment: a case-study along the Syowa–Mizuho–Dome Fuji traverse, Ann. Glaciol., 34, 157–164, 2002.

Fujita, S., Holmlund, P., Andersson, I., Brown, I., Enomoto, H., Fujii, Y., Fujita, K., Fukui, K., Furukawa, T., Hansson, M., Hara, K., Hoshina, Y., Igarashi, M., Iizuka, Y., Imura, S., Ingvander, S., Karlin, T., Motoyama, H., Nakazawa, F., Oerter, H., Sjöberg, L. E., Sugiyama, S., Surdyk, S., Ström, J., Uemura, R., and Wilhelms, F.: Spatial and temporal variability of snow accumulation rate on the East Antarctic ice divide between Dome Fuji and EPICA DML, The Cryosphere, 5, 1057–1081, doi:10.5194/tc-5-1057-2011, 2011.

Goodwin, I. D.: Snow accumulation and surface topography in the katabatic zone of eastern Wilkes Land, Antarctica, Antarct. Sci., 2, 235–242, 1990.

Gow, A. J. and Rowland, R.: On the relationship of snow accumulation to surface topography at “Byrd Station”, Antarctica, J. Glaciol., 5, 843–847, 1965.

Gregory, S. A., Albert, M. R., and Baker, I.: Impact of physical properties and accumulation rate on pore close-off in layered firn, The Cryosphere, 8, 91–105, doi:10.5194/tc-8-91-2014, 2014.

Hamilton, G. S.: Topographic control of regional accumulation rate variability at South Pole and implications for ice-core interpretation, Ann. Glaciol., 39, 214–218, 2004.

Karlöf, L., Winebrenner, D. P., and Percival, D. B.: How representative is a time series derived from a firn core? A study at a low-accumulation site on the Antarctic Plateau, J. Geophys. Res., 111, 1–11, 2006.

Kaspari, S., Mayewski, P. A., Dixon, D. A., Spikes, V. B., Sneed, S. B., Handley, M. J., and Hamilton, G. S.: Climate variability in West Antarctica derived from annual accumulatiuon-rate records from ITASE firn/ice cores, Ann. Glaciol., 39, 585–594, 2004.

Landais, A., Ekaykin, A. A., Barkan, E., Winkler, R., and Luz, B.: Seasonal variations of ^{17}O-excess and d-excess in snow precipitation at Vostok Station, East Antarctica, J. Glaciol., 58, 725–733, 2012.

Lenaerts, J. T. M., van den Broeke, M. R., Déry, S. J., König-Langlo, G., Ettema, J., and Munneke, P. K.: Modelling snowdrift sublimation on an Antarctic ice shelf, The Cryosphere, 4, 179–190, doi:10.5194/tc-4-179-2010, 2010.

Mahalinganathan, K., Thamban, M., Laluraj, C. M., and Redkar, B. L.: Relation between surface topography and sea-salt snow chemistry from Princess Elizabeth Land, East Antarctica, The Cryosphere, 6, 505–515, doi:10.5194/tc-6-505-2012, 2012.

Neumann, T. A., Waddington, E. D., Steig, E. J., and Grootes, P. M.: Non-climate influences on stable isotopes at Taylor Mouth, Antarctica, J. Glaciol., 51, 248–258, 2005.

Oerter, H., Wilnelms, F., Jung-Rothenhausler, F., Goktas, F., Miller, H., Graf, W., and Sommer, S.: Accumulation rates in Dronning Maud Land, Antarctica, as revealed by dielectric-profiling measurements of shallow firn cores, Ann. Glaciol., 30, 27–34, 2000.

Pettre, P., Pinglot, F., Pourchet, M., and Reynaud, L.: Accumulation distribution in Terre Adelie, Antarctica: effect of meteorological parameters, J. Glaciol., 32, 486–500, 1986.

Popov, S. V. and Eberlein, L.: Investigation of snow-firn thickness and ground in the East Antarctica by means of geophysical radar, Led i Sneg, 4, 95–106, 2014.

Popov, S. V. and Masolov, V. N.: Forty-seven new subglacial lakes in the 0–110*E sector of East Antarctica, J. Glaciol., 53, 289–297, 2007.

Richardson, C., Aarholt, E., Hamran, S.-E., Holmlund, P., and Isaksson, E.: Spatial distribution of snow in western Dronning Maud Land, East Antarctica, mapped by a ground-based snow radar, J. Geophys. Res., 102, 20343–20353, 1997.

Richter, A., Fedorov, D. V., Fritsche, M., Popov, S. V., Lipenkov, V. Y., Ekaykin, A. A., Lukin, V. V., Matveev, A. Y., Grebnev, V. P., Rosenau, R., and Dietrich, R.: Ice flow velocities over Vostok Subglacial Lake, East Antarctica, determined by 10 years of GNSS observations, J. Glaciol., 59, 315–326, doi:10.3189/2013JoG12J056, 2013.

Rotschky, G., Eisen, O., Wilhelms, F., Nixdorf, U., and Oerter, H.: Spatial distribution of surface mass balance on Amundsenisen Plateau, Antarctica, derived from ice-penetrating radar studies, Ann. Glaciol., 39, 265–270, 2004.

Scambos, T. A., Frezzotti, M., Haran, T. V., Bohlander, J., Lenaerts, J. T. M., Van den Broeke, M. R., Jezek, K., Long, D., Urbini, S., Farness, K., Neumann, T., Albert, M., and Winther, J.-G.: Extent of low-accumulation "wind-glaze" areas on the East Antarctic Plateau: implications for continental ice mass balance, J. Glaciol., 58, 633–647, 2012.

Schoenemann, S. W., Schauer, A. J., and Steig, E. J.: Measurement of SLAP2 and GISP δ^{17}O and proposed VSMOW-SLAP normalization for δ^{17}O and ^{17}O$_{\text{excess}}$, Rapid Commun. Mass Spectrum., 27, 582–590, 2013.

Severinghaus, J. P., Albert, M. R., Courville, Z. R., Fahnestock, M. A., Kawamura, K., Montzka, S. A., Muhle, J., Scambos, T. A., Shields, E., Shuman, C. A., Suwa, M., Tans, P., and Weiss, R. F.: Deep air convection in the firn at a zero-accumulation site, central Antarctica, Earth Planet. Sc. Lett., 293, 359–367, 2010.

Swithinbank, C.: Antarctica, US Geol. Survey Prof. Rap. 1386-B, US Geological Survey, Washington, D.C., 1988.

Thiery, W., Gorodetskaya, I. V., Bintanja, R., Van Lipzig, N. P. M., Van den Broeke, M. R., Reijmer, C. H., and Kuipers Munneke, P.: Surface and snowdrift sublimation at Princess Elisabeth station, East Antarctica, The Cryosphere, 6, 841–857, doi:10.5194/tc-6-841-2012, 2012.

Town, M. S., Warren, S. G., Walden, V. P., and Waddington, E. D.: Effect of atmospheric water vapor on modification of stable isotopes in near-surface snow on ice sheets, J. Geophys. Res., 113, 1–16, 2008.

Van der Veen, C. J., Mosley-Thompson, E., Gow, A., and Mark, B. G.: Accumulation at South Pole: comparison of two 900-year records, J. Geophys. Res., 104, 31067–31076, 1999.

Vladimirova, D. O. and Ekaykin, A. A.: Climatic variability in Davis Sea sector (East Antarctica) over the past 250 years based on the "105 km" ice core geochemical data, Geophys. Res. Abstr., 16, 285, 2014.

Whillans, I. M.: Effect of inversion winds on topographic detail and mass balance on inland ice sheets, J. Glaciol., 14, 85–90, 1975.

Zwally, H. J., Li, J., Robbins, J. W., Saba, J. L., Yi, D., and Brenner, A. C.: Mass gains of the Antarctic ice sheet exceed losses, J. Glaciol., 61, 1019–1036, doi:10.3189/2015JoG15J071, 2015.

Table 1. Glaciological, radio-echo-sounding and geodetic data used in this study.

Point name	Distance from MD00 (m)	Altitude a.s.l. (m)	Stake height (cm)		Snow build-up (cm)	Mean snow density ($g\,cm^{-3}$)	Snow accumulation (mm we)	Isotope content 58 RAE				Depths of internal reflection horizons (m)						
			58 RAE	60 RAE				δD	$\delta^{18}O$	dxs	17O-excess	1st	2nd	3rd	4th	5th	6th	7th
MD00	0	3424.25	300	292	4	0.358	14	−434.3	−56.04	14.0	−5	4	8	11	14	17	19	24
MD01	88	3424.92	151	152	−0.5	0.311	−2	−437.9	−56.37	13.1	−13	6	9	12	15	18	20	25
MD02	192	3425.75	172	163	4.5	0.330	15	−436.3	−56.30	14.1	−16	7	10	13	16	18	20	25
MD03	291	3426.37	170	170	0	0.338	0	−432.8	−55.76	13.3	−6	8	11	14	17	19	20	26
MD04	393	3427.09	195	190	2.5	0.355	8	−441.5	−56.97	14.3	−9	10	12	15	17	18	19	27
MD05	493	3427.86	175.5	165	5.25	0.367	20	−434.0	−55.97	13.8	−19	11	13	15	17	18	19	28
MD06	592	3428.35	169	167	1	0.335	3	−435.8	−56.36	15.1	−16	11	13	15	16	17	18	28
MD07	690	3428.51	171.5	154	8.75	0.345	32	−444.7	−57.49	15.2	−13	11	13	14	16	17	18	28
MD08	797	3428.73	193.5	177	8.25	0.346	28	−446.9	−57.94	16.5	−13	11	13	14	15	16	17	28
MD09	894	3428.65	187.5	170	8.75	0.345	31	−442.0	−57.29	16.3	−9	10	12	13	14	15	17	27
MD10	992	3428.61	169.5	150	9.75	0.370	34	−441.2	−57.02	15.0	0	9	12	13	14	15	17	27
MD11	1066	3428.44	179	146	16.5	0.363	57	−445.1	−57.47	14.7	−9	8	10	12	14	14	16	26
MD12	1168	3428.18	162	148	7	0.330	21	−442.7	−57.27	15.5	3	7	9	11	13	14	16	25
MD13	1289	3427.64	190.5	158	16.25	0.344	55	−436.5	−56.32	14.0	−12	5	8	11	13	14	16	24
MD14	1394	3427.53	204	188	8	0.360	28	−435.2	−56.08	13.4	2	4	8	11	13	14	17	23
MD15	1493	3427.53	196	178	9	0.337	28	−428.6	−55.17	12.8	−8		8	12	14	15	17	23
MD16	1593	3427.76	171	165	3	0.385	11	−425.0	−54.62	11.9	0		9	13	15	16	18	23
MD17	1698	3428.17	157	140	8.5	0.435	32	−432.1	−55.51	11.9	−15		10	14	16	17	19	24
MD18	1796	3428.73	188	178	5	0.348	18	−435.5	−56.04	12.8	−9	3	12	15	17	18	19	25
MD19	1901	3429.6	209	201	4	0.420	13	−440.4	−56.72	13.3	8	4	13	16	18	19	20	26
MD20	1983	3430.17	184.5	172	6.25	0.335	19	−437.8	−56.38	13.3	−10	10	15	18				29

Title Page
Abstract | Introduction
Conclusions | References
Tables | Figures
◀| |▶
◀ ▶
Back | Close
Full Screen / Esc
Printer-friendly Version
Interactive Discussion

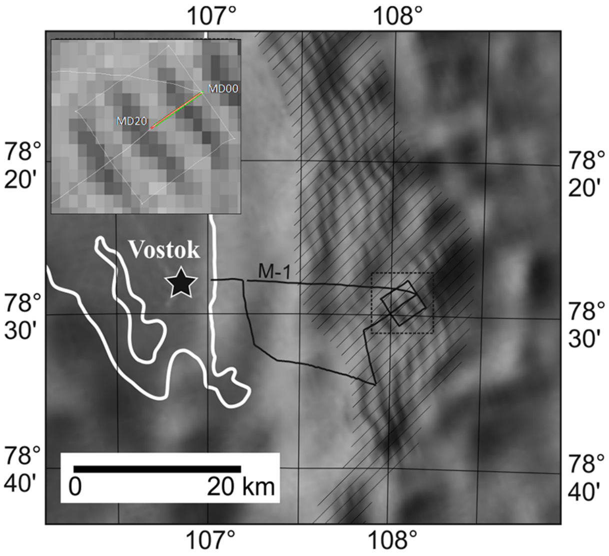

Figure 1. Vicinities of Vostok Station and the location of the study area. The mega-dunes are highlighted by hatching. Black line is the route of GPR and geodetic profiles. The location of the glaciological profile is shown in the insert (MD00-MD20). White line is the Vostok lake shoreline adapted from Popov and Masolov (2007).

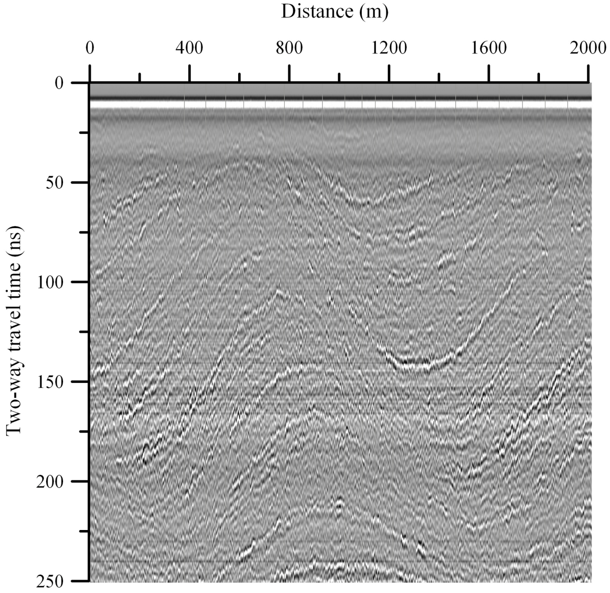

Figure 2. GPR registration recorded along the MD00 profile.

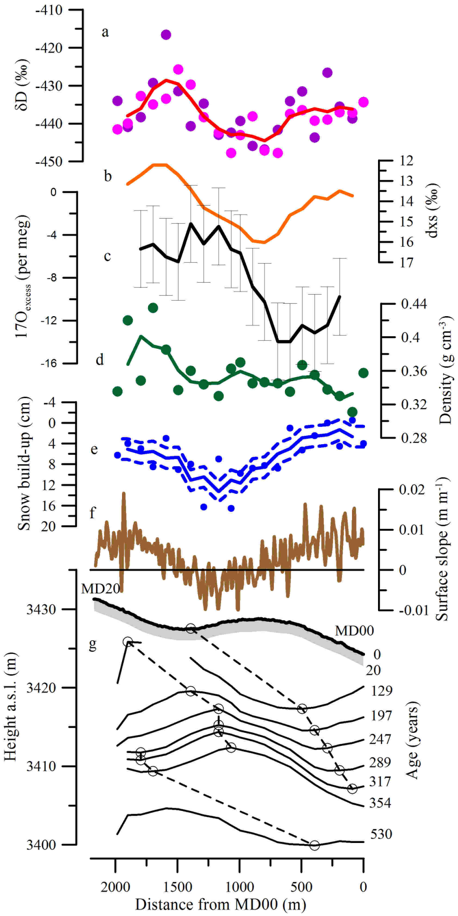

a
b
c
d
e
f
g
δD (‰)
-410
-420
-430
-440
-450
12
13
14
15
16
17
dxs (‰)
0
-4
-8
-12
-16
17O$_{excess}$ (per meg)
0.44
0.4
0.36
0.32
0.28
Density (g cm^{-3})
-4
0
4
8
12
16
20
Snow build-up (cm)
0.02
0.01
0
-0.01
Surface slope (m m^{-1})
MD20
MD00
3430
3420
3410
3400
Height a.s.l. (m)
0
20
129
197
247
289
317
354
530
Age (years)
2000
1500
1000
500
0
Distance from MD00 (m)

Figure 3. The results of the glaciological, GPR and geodetic survey in the Vostok mega-dune area. **(a–c)** Isotopic content of the surface (1.5 m) layer of the snow thickness, δD **(a)**, dxs **(b)** and 17O-excess **(c)**. For δD the points show the individual samples and the red line is the average of the 58 and 59 RAE samples. For dxs only the average is shown. Note that the dxs axis is reversed. For 17O-excess we showed the 5-point running means with the error bars ($\pm 1\sigma$, where σ is the error of the average of 5 individual values). **(d)** Surface (20 cm) snow density, individual values (points) and 3-point running mean (line). **(e)** Mean snow build-up in 2013–2014, individual values (points) and 3-point running mean. Dashed lines show the confidence interval ($\pm 1\sigma$) of 2-year average accumulation value as deduced from Vostok stake network. Note that the Y axis is reversed. **(f)** Surface slope calculated over 20 m intervals of the ice sheet surface. Negative values mean that the local slope is the opposite of the general slope in this region (from south-west to north-east). **(g)** The elevation of the ice sheet surface and of 7 internal reflection horizons (IRH) above sea level defined by the geodetic measurements and GPR survey. The gray shading depicts the snow layer (1.5 m) in which the snow isotopic content was measured. The dashed lines connect the fold hinges used to calculate the dune drift velocity. The values to the right are the estimated ages of each IRH relative to January 2015. The profile is spread from south-west (left part of the figure) to the north-east (right part), see Fig. 1. The individual values shown in Fig. 3 can be found in Table 1.

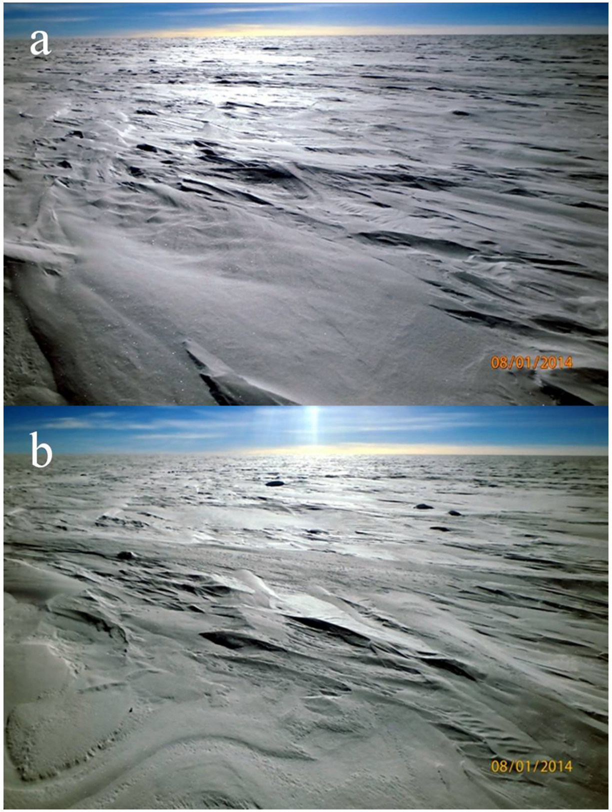

Figure 4. Photo of the snow surface in points MD02 **(a)** – erosion zone, leeward slope of the dune – and MD13 **(b)** – deposition zone, the hollow between dunes.

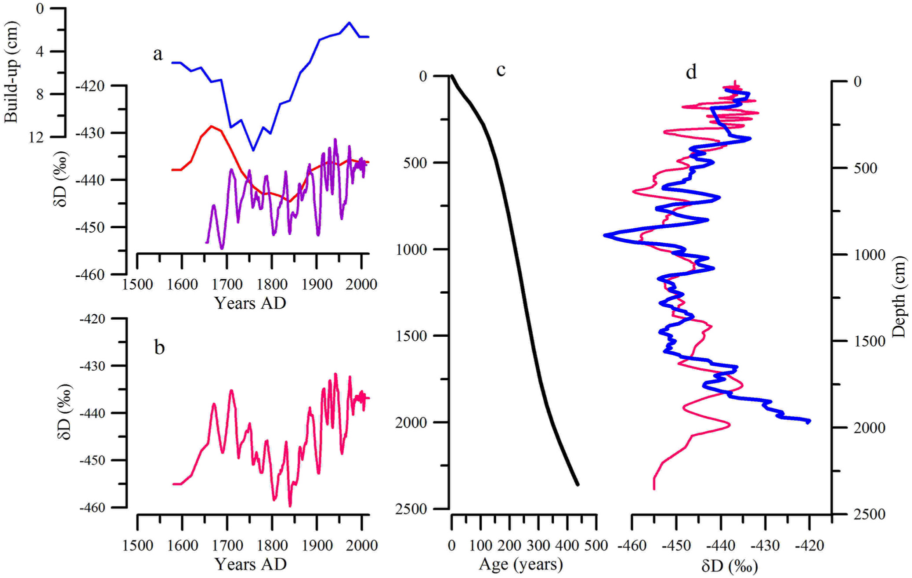

Figure 5. Simulated isotope profile in MD00 point. **(a)** The values of snow accumulation rate (blue) and isotopic composition (red) that could be observed in point MD00 if one would measure them as long as the dune travel across this point. To calculate this we used the data from Fig. 3a and e, and data on the dune drift velocity. Purple – climatic variability of the snow isotopic composition in the Vostok region taken from Ekaykin et al. (2014). **(b)** A combination of climatic and dune-related isotopic variability (red + purple from Fig. 5a). **(c)** Depth-age function for the snow thickness in point MD00. **(d)** Simulated vertical profile of snow isotopic composition calculated using the data from Fig. 5b and depth-age function (Fig. 5c), in red, compared with the real vertical profile of snow isotopic composition measured in the core drilled in point MD00, in blue.